


John, S., Shivdasani, M. N., Leuenberger, J., Fallon, J., Shepherd, R., Millard, R., Rathbone, G. D., & Williams, C. E. (2011). An automated system for rapid evaluation of high-density electrode arrays in neural prostheses. *Journal of Neural Engineering, 8*(3), Article#036011.



**http://dx.doi.org/10.1088/1741-2560/8/3/036011**

# An automated system for rapid evaluation of high density electrode arrays in neural prostheses

Running Head: An automated system for rapid evaluation of high density electrode arrays

Sam E John[1,2], Mohit N Shivdasani[1], James Leuenberger[1,4], James B Fallon[1,3], Robert K Shepherd[1,3], Rodney E Millard[1], Graeme D Rathbone[1,2], and Chris E Williams[1,3].

[1]The Bionic Ear Institute, Daly Wing, St Vincent's Hospital, VIC – 3065, AUSTRALIA

[2]Department of Electronic Engineering, La Trobe University, VIC – 3086, AUSTRALIA

[3]Department of Otolaryngology, University of Melbourne, Royal Victorian Eye and Ear Hospital, VIC – 3002, AUSTRALIA

[4]University of Bern, CH – 3012, Bern, Switzerland

[5]Corresponding Author:

*A Prof.* Chris E Williams

The Bionic Ear Institute, 6th Floor, Daly Wing, St Vincent's Hospital, Fitzroy, VIC – 3065, AUSTRALIA.

Tel: +61-3-92883523

Fax: +61-3-92882998

Email: cwilliams2@bionicear.org

## Abstract

The success of high density electrode arrays for use in neural prostheses depends on efficient impedance monitoring and fault detection. Conventional methods of impedance testing and fault detection are time consuming and are not always suited for *in-vivo* assessment of high density electrode arrays. Additionally the ability to evaluate impedances and faults such as open and short circuits both, *in-vitro* and *in-vivo* are important to ensure safe and effective stimulation.. In the present work we describe an automated system for the rapid evaluation of high density electrode arrays. The system uses a current pulse similar to that used to stimulate neural tissue and measures the voltage across the electrode in order to calculate the impedance. The switching of the system was validated by emulating a high density electrode array using light emitting diodes and a resistor-capacitor network. The system was tested *in-vitro* and *in-vivo* using a range of commercially available and in-house developed electrode arrays. The system accurately identified faults on an 84 electrode array in less than 20 seconds and reliably measured impedances up to 110 kΩ using a 200 μA, 250 μs per phase current pulse. This system has direct application for screening high density electrode arrays in both a clinical and experimental setting.

## 1. Introduction

High density electrode arrays are being used in neural prostheses in several chronic recording and electrical stimulation applications (Brindley and Lewin, 1968, Rizzo et al., 2003, Prochazka and Mushahwar, 2004, Schwartz, 2004, Mccreery et al., 2006, Donoghue, 2008, Middlebrooks and Snyder, 2008). However, the success of such devices depends on several factors including: access to a large number of electrically active electrodes; rapid electrode switching and effective mapping of stimuli to multiple electrodes on the array; estimation of the instantaneous impedance of the electrode-tissue interface; and quick and reliable electrode fault detection. For chronic neural prostheses, the instantaneous impedance describes the functional ability of the electrode.

Impedance spectroscopy, the sine wave method (SWM) and the stimulus waveform test (SWT) have commonly been used to measure impedances of electrodes in neural prostheses (table 1). Impedance spectroscopy uses a low voltage sinusoidal input (10-50 mV) and provides the phase angle and magnitude of the impedance over a range of frequencies. Impedance spectroscopy can characterize the impedance dominated by the electrode from the impedances measured at high frequencies and the impedance dominated by tissue reaction (e.g. encapsulation) from the impedances measured at low frequencies (Mercanzini et al., 2009). However, impedance spectroscopy requires the use of a wide range of frequencies and is time consuming.

The SWM uses a low voltage or current sinusoidal input (10-50 mV / 1-20 nA) and reports the impedance at 1 kHz (Hornig et al., 2005, Gunalan et al., 2009). The 1 kHz frequency is used because it roughly corresponds to the 1 ms duration of the neuron's action potential (Mercanzini et al., 2009). Gunalan et al. (2009) describe an automated system for evaluating high density electrode arrays using this method. They used a 10 mV, 1 kHz sine wave to evaluate the impedance of a 100 electrode array in 5 minutes with a three electrode set up (working, reference and counter). However, the SWM is less relevant for applications involving electrical stimulation as it does not differentiate between the impedance of the tissue reaction and the impedance of the electrode and

the tissue surrounding it (Mercanzini et al., 2009). As a result the SWM is more suited for assessing recording electrodes (Cogan, 2008). In addition both the SWM and impedance spectroscopy use low voltage or current levels and do not replicate the clinically relevant levels used for neural stimulation.

There is therefore a need to monitor impedance using clinically relevant stimulus pulses and current levels. In addition, it would be advantageous for such a method to provide an estimate of the current that can be safely injected into tissue; confirm that the stimulator is working within its designed voltage compliance for a given current; provide an estimate of the charge balanced state of the current pulse; and provide an indication of the tissue reactions around the electrode. The SWT uses a bi-phasic or mono-phasic constant current pulse, similar to those used to stimulate neural tissue. In the present work, a charge balanced symmetric bi-phasic constant current pulse was used to measure impedance under clinically relevant conditions (Weinman and Mahler, 1964, Brummer and Turner, 1977, Parker et al., 1999, Tykocinski et al., 2005, Cogan, 2008). Using this method both the current and voltage waveforms can be monitored, enabling one to confirm that there is no imbalance in the current waveforms and that the stimulator is working within its compliance limits for the given stimulus parameters. In addition, the SWT can give an indication of the tissue reactions in the vicinity of the electrode due to stimulation (Shepherd et al., 1990, Xu et al., 1997, Newbold et al., 2004). Xu et al. (1997) and Newbold et al. (2004) showed that there is a direct correlation between tissue reaction (such as fibrous tissue growth around the electrode) and impedance. If the impedance becomes too high the stimulator may begin to operate out of voltage compliance which may lead to loss of charge balance, resulting in tissue damage (Seligman and Shepherd, 2004). Reducing irreversible electrochemical reactions and ensuring charge balance are essential in providing safe neural stimulation (Brummer and Turner, 1977, Seligman and Shepherd, 2004). We describe a fully isolated flexible system that allows the user to: connect an electrode or a combination of electrodes on the array as the stimulating (active) or the return electrode(s);

measure impedances in different configurations; and detect faults on the array such as open circuits and short circuits.

**Table 1.** Impedance properties of commonly used electrode arrays and materials

| **Application** | **Auditory Prosthesis** | **Visual Prosthesis** | **Visual Prosthesis** | **Visual Prosthesis** | **Motor Prosthesis** | **Brain-Machine interfaces** |
|---|---|---|---|---|---|---|
| **Species** | Human | Human | Cat | Rabbit | Cat | Monkey |
| **Electrode Placement** | Cochlea | Epiretinal | Supra-choroidal | Subretinal | Spinal cord | Primary Motor Cortex |
| **Application Array configuration** | Stimulation 24 | Stimulation 4 × 4 | Stimulation 6 ×12 | Stimulation 3 × 5 | Stimulation 6 to 12 wires | Recording 10x10 |
| **Electrode Electrode Material** | Full banded Platinum | Surface Sputtered thin film platinum | Surface Plated Platinum | Surface Activated iridium oxide | Penetrating Stainless-steel wires | Penetrating Boron-doped silicon shanks with Pt-coated Tips |
| **Geometric Surface areas** | 480000 $\mu m^2$ to 300000 $\mu m^2$ | 31415 $\mu m^2$ to 1963 $\mu m^2$ | 123000 $\mu m^2$ to 20100 $\mu m^2$ | 125600 $\mu m^2$ | 3000 $\mu m^2$ to 1400 $\mu m^2$ | 1600 $\mu m^2$ |
| **Mean *in-vitro* Impedance** | 0.2-1.5 kΩ | Not reported | 2-20 kΩ Saline | 3.6 kΩ at 1kHz Interstitial fluid (ISF) | 10-30 kΩ | 100–750 kΩ saline |
| **Mean *in-vivo* Impedance** | 1-12 kΩ | 10 -100 kΩ at 1 kHz | 20-50 kΩ | 3.8 kΩ at 1 kHz | Not reported | 50-1000 kΩ |
| **Method used to measure impedance** | SWT-Stimulus Waveform Test | Electrochemical Impedance Spectroscopy: 10 mV sine wave; 10-100 kHz. | SWT-Stimulus Waveform Test | Electrochemical Impedance Spectroscopy: 10 mV sine wave; 10-100 kHz. | Not reported | Sine Wave method: 1 nA, 1 kHz sine wave |
| **References** | (Shepherd et al., 1990, Tykocinski et al., 2005) | (Shah et al., 2007) | (Shivdasani et al., 2010) | (Cogan, 2006) | (Mushahwar et al., 2000) | (Suner et al., 2005) |

## 2. Material and methods

### *2.1. Hardware and Software Design*

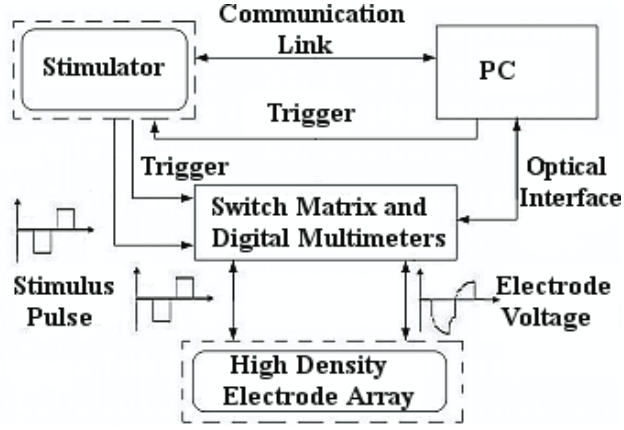


*Figure 1: Hardware block diagram of the system consists of a personal computer (PC), a constant current stimulator, two Digital Multimeters (DMMs) and a cross-point switch matrix. The DMMs, switch matrix and stimulator were isolated to ensure safety of the experimental animals and for clinical use. The dotted lines indicate components which can be easily replaced with alternative components. Biphasic stimulation pulses were routed to the electrode array via the cross-point switch matrix. The current and voltage responses were recorded and measured using the DMMs and were displayed on the PC.*

Figure 1 shows a schematic diagram of our system, the dotted lines indicate components which can be easily replaced with commercially available or custom built components. The basic components consist of a National Instruments 512 cross-point reed relay switch matrix (NI PXI-2532; NI, Austin TX) and two NI isolated digital multimeters (DMMs, NI PXI-4072) in a PXI chassis. The NI-2532 switch matrix has a maximum switching speed of 2,000 cycles/sec with a relay operating time of 0.25 ms, relay release time 0.25 ms, switch settling time up to 3.4 ms and NI-4072 DMM is

a high accuracy digitizer with an initialisation time of 4 ms. One DMM was connected in series with the stimulator and measured the stimulus current waveform. The second DMM was connected in parallel to the electrode array via the switch matrix and measured the voltage across the electrode(s). A personal computer was connected to the PXI chassis through a NI MXI-4 optical interface. An optically isolated constant current stimulator (Shepherd et al., 1990) developed in-house was used to provide the stimulation current. The stimulator was shorted at the end of each pulse to minimize any direct current. The stimulator output was fed to the electrode array through a pair of ribbon cables via the switch matrix.

Custom software (virtual instrument, VI) was developed in LabVIEW to synchronize and control the data acquisition and online analysis of the data. The user can enter the stimulus pulse parameters, electrode configuration to test, electrode area and the safe maximum charge-density (Rose and Robblee, 1990) for the given electrode array. The VI uses the entered pulse parameters to calculate the charge that would be injected through the electrode. The VI automatically aborts the test if the calculated charge exceeds the maximum charge-injection capacity for the electrode. Both the current and voltage waveforms were acquired by the DMMs. The acquired waveforms are then filtered using LabVIEW and the raw and analysed data were displayed on the PC.

### *2.2. Stimulation Pattern Mapping*

Monopolar configurations are widely used for neural stimulation (Weiland and Anderson, 2000, Clark, 2003, Shivdasani et al., 2010). This configuration uses a single or a combination of electrode(s) as the active and a remote electrode as the return. The common ground configuration is another electrode configuration which has been implemented in the Nucleus 22 channel cochlear implant (Cochlear Ltd) (Clark, 2003). In this configuration, one electrode on the array acts as the active electrode and all other electrodes on the array form the return. Recent advances in visual

prosthesis have motivated the investigation of several patterns of stimulations (Humayun et al., 1999, Xinyu et al., 2008) such as squares, lines (rows and columns), letters and circles (Zrenner et al., 2010). Furthermore, the need to improve spatial resolution has led researchers to investigate patterns such as bipolar stimulation and the hexagonal return configuration(Suaning et al., 2004). The system was used to implement some of these commonly used electrode configurations. Figure 2 shows schematic examples of some stimulation configurations created on an 84 electrode platinum plated array designed in-house (Shivdasani et al., 2010).

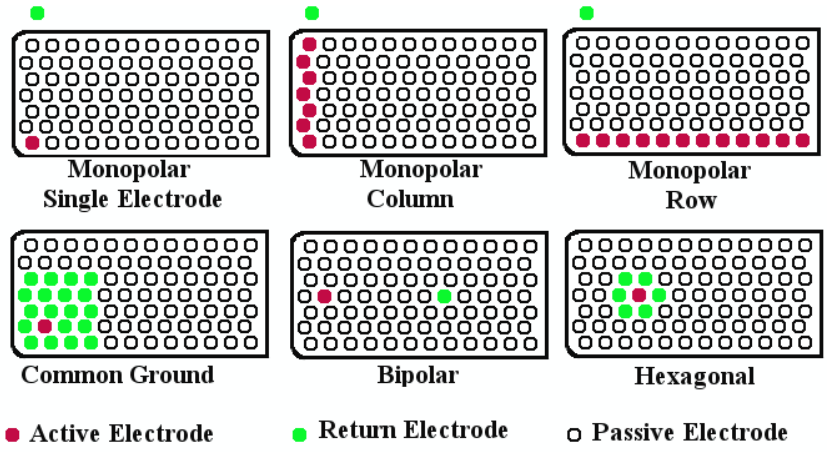


*Figure 2: Examples of electrode configurations. Upper: monopolar configurations using a remote return electrode; single electrode (SE), monopolar row (ROW) and monopolar column (COL). Lower: common ground (CG), bipolar electrode pair (BP) and hexagonal return (HX). These maps were visually verified on an LED emulation of the platinum plated array.*

1) Monopolar Single Electrode (SE): Used one electrode on the array as the active electrode and a remote electrode as the return electrode.

2) Monopolar column (COL): Used a column of electrodes on the array shorted together as the active electrode and a remote electrode as the return electrode.
3) Monopolar row (ROW): Used a row of electrodes on the array shorted together as the active electrode and a remote electrode as the return electrode.
4) Common ground (CG): Used one electrode on the array as the active electrode and the 19 electrodes closest to it on the array were shorted together as the return electrode.
5) Bipolar pair (BP): Used one electrode on the array as the as the active electrode and a second electrode on the array as the return electrode.
6) Hexagonal return (HX): Used one electrode on the array as the central active electrode and the six electrodes surrounding it were shorted together as the return electrode (Suaning et al., 2004).

A platinum ball electrode (1.5 mm diameter) with an impedance of 350 Ω was used as the remote return electrode for monopolar stimulation. The platinum ball electrode was placed in the vitreous humour during the *in-vivo* experiments and in normal saline (0.9% NaCl) during *in-vitro* experiments. *In-vivo* studies were approved by the Royal Victorian Eye and Ear Hospital Animal Ethics Committee.

### *2.3 Impedance Testing Procedure*

The impedance measurements used a two electrode set up (active and return) and different electrode configurations as described in section 2.2. The system acquired the current waveform (figure 3A) from the stimulator and the voltage waveform (figure 3B) across the electrode. The acquired waveforms were filtered with a median filter of rank 7 to remove the large current spikes caused by shorting the stimulator and stray capacitance. It was important to eliminate spikes in the acquired waveforms to ensure accuracy and a spatial filter such as the median filter effectively

eliminated impulse noise such as current spikes. The rank of the median filter is number of samples used to compute the median filter and the data sampled at 1.8 M Samples/second. Both the current pulse and the resultant electrode voltage waveforms acquired are analogous to periodic square pulses. These square pulses can be analysed as an initial step which corresponds to a high frequency AC sinusoidal wave followed by a plateau which corresponding to zero frequency (Teorell, 1946). In this case the impedance is the ratio of the potential difference across the electrode-tissue interface to the current flowing through it (Dymond, 1976).

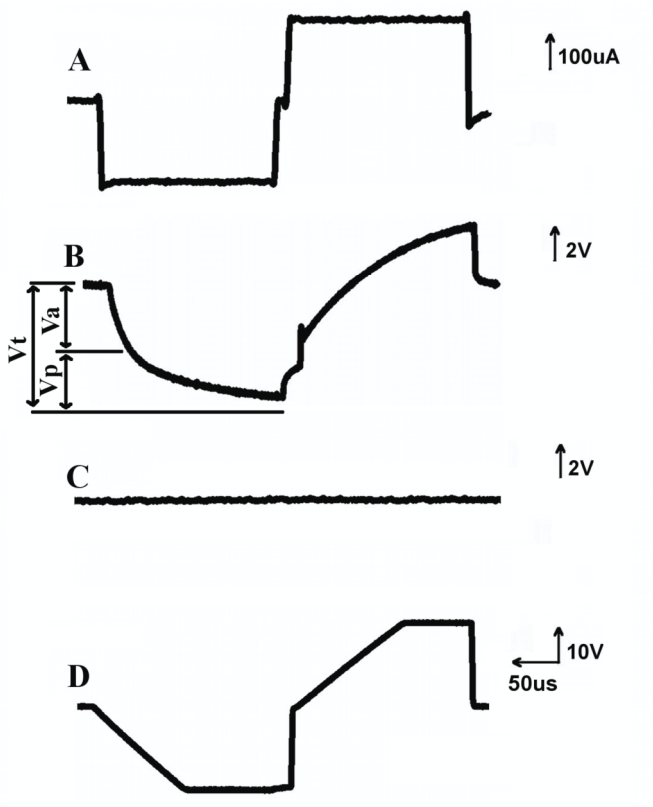


*Figure 3: A biphasic current stimulation pulse injected through a working, short circuit and an open circuit electrode along the corresponding voltage waveform recorded by the system. (A) A*

*charge balanced biphasic constant current pulse (200µA, 250µs per phase, 25µs interphase gap) was used for stimulation and was recorded by the first DMM. (B) The monopolar-single electrode voltage across the electrode was recorded by the second DMM. The waveform shows the electrode had a total impedance of 15 kΩ and a peak voltage of 3.2 V which was within the operational range for the stimulator. (C) The common ground voltage across an electrode that was shorted to one of its neighbouring 19 electrodes (the neighbouring19 electrodes form the return electrode in the CG configuration) on the array. (D) The monopolar-single electrode voltage across an electrode that was found to be open circuited. Note: Different scale for D.*

The impedance was calculated from the peak current and peak voltage [Vt] obtained from the leading cathodic phase (figure 3A and 3B). The overall impedance [Zt] using the SWT represents the sum of the bulk impedance [Za] and the polarization impedance [Zp]. The bulk impedance [Za] results in the initial steep rise in the voltage [Va] in figure 3A and the polarization impedance [Zp] is due to the slow rising voltage reaching its peak [Vp] level in figure 3A (Tykocinski et al., 2005). It is suggested that the bulk impedance is dominated by the resistivity of the electrode and the tissue surrounding it, while the polarization impedance is dominated by the electrochemical electrode-tissue interface. For the purpose of this paper all impedances reported in this study are total impedances [Zt].

*2.4 System Validation and Testing*

The working range and accuracy of the system were characterized using a resistor-capacitor (RC) network. The RC network was constructed to emulate the electrode-tissue interface (inset of figure 4), $R_A$ was kept constant at 1.1 kΩ, C was varied in the nF range and $R_X$ was varied in the kΩ-MΩ range using 20 different combinations (Seligman and Shepherd, 2004). For each combination we

calculated the theoretical equivalent impedance ($Z_{eq}$) of the circuit model using, $Z_{eq}= Z_A+ (Z_X||Z_C)$, where, $Z_A = R_A$, $Z_X = R_X$ and $Z_C = X_C$ ($X_C$ is the capacitive reactance of the capacitor at a given frequency f= (1/T), where T is the pulse width of the leading phase of the stimulus used) (Dymond, 1976). In addition, tests were performed to evaluate the effect of changes in current amplitude and pulse width on measured impedance. Three RC circuits were built using the circuit diagram in inset of figure 4 to represent the low, middle and high measurement ranges of the system. In the first test the pulse width was kept constant at 250 μs per phase pulse and the current was varied between 10-200 μA. In the second test the current was kept constant at 200 μA and the pulse width was varied between 50-1000 μs per phase, except in the highest range of impedance where the stimulator reached compliance at 400 μs per phase and only pulse widths up to 200 μs per phase are reported for this impedance range.

Two in-house developed arrays made of pure platinum and plated platinum and one commercially available array made of iridium oxide were tested *in-vitro* in normal saline:

1. Pure platinum array: A feline version of the scala tympani electrode array (Shepherd et al., 1983), comprising of eight platinum (Pt) ring electrodes was used. The scala tympani electrode array had the largest geometrical surface area (GSA) of 430000 $\mu m^2$.

2. Platinum plated array: A platinum plated array was designed in-house and manufactured by Flexible Circuit Technologies (Plymouth, MN). It comprised of a polyimide substrate with platinum plated-gold disc electrodes(Shivdasani et al., 2010). The electrodes had a GSA of 123000 $\mu m^2$ and were arranged in a 7 row x 12 electrode configuration.

3. Iridium oxide array: A 32 electrode activated iridium oxide multichannel array was purchased from NeuroNexus Technologies Inc. (Ann Arbour, MI). The iridium oxide array was arranged in a 4 row x 8 electrode configuration and each electrode had a GSA of 413 $\mu m^2$.

The impedances of all individual electrodes on each array were measured with the SWT against a platinum ball return electrode in the monopolar single electrode configuration. The impedances obtained with the system were compared to those obtained using the SWM (Solartron 1260 impedance gain-phase analyser and the Solartron 1287 electrochemical interface Solartron Analytical, Hampshire UK). The SWM was performed with a three electrode set up with a platinum wire as the counter; a saturated Ag|AgCl as the reference electrode and the working electrode as the array being tested. The three electrodes were immersed in normal saline at room temperature and a 4 kHz, 10 mV sine wave was applied. This frequency was chosen as it roughly corresponds to the nominal frequency of the current pulse used in the current work.

The electrode configurations were verified visually on an emulation of the platinum plated electrode array made of light emitting diodes (LED) configured as in figure 2. Red and green LEDs were connected in opposite directions to display each stimulation phase. The system's ability to test electrodes *in-vitro* and *in-vivo* in different configurations was verified with the platinum plated array (section 3.2). The *in-vitro* impedances were obtained with the array in normal saline before implantation and *in-vivo* impedances were obtained post-operatively in the suprachoroidal space of cats (Shivdasani et al., 2010). The mean *in-vitro* impedance in each configuration was compared to its corresponding mean *in-vivo* impedance.

### *2.5 Fault Detection*

The impedance of the electrodes was also used to determine faults on the array such as short circuits (using CG configurations) and open circuits (using SE or CG configurations). Short circuits can exist between the active electrode and its neighbouring electrodes on the array due to fluid leaking into the substrate forming an electrical short circuit or wiring errors. In the present work,

the common ground configuration comprised an active electrode and a return electrode incorporated 19 electrodes closest to the active electrode. Short circuits were detected when the electrodes forming the short showed identical low impedances (< 300 Ω) and the peak voltage was close to zero indicating the noise floor (figure 3C). Open circuits can be formed by corrosion of the electrode surface; dissolution of the electrode material; breakage of the lead wires or wiring errors. Open circuits were identified when the electrode showed high impedance and a voltage waveform with a peak voltage equal to the stimulator compliance limit (24 V for our lab stimulator) (figure 3D). If an electrode(s) on the array is found to be faulty that electrode can be excluded from the stimulating configuration.

Several tests were performed to evaluate the system's ability to detect faults. First, a platinum plated array was modified to deliberately produce faults: five tracks on the array were cut and five pads were coated with silicone to form open circuits; while three pairs of electrode were soldered together to form short circuits. This array was then tested *in-vitro* in normal saline. Second, to ensure that the system could identify faults *in-vivo*, platinum plated arrays were tested during several acute visual prosthesis experiments in the suprachoroidal space of a cat (Shivdasani et al., 2010). Prior to implantation each platinum plated array was visually inspected for faults, this was followed by impedance measurements *in-vitro* in normal saline and *in-vivo* in the suprachoroidal space of a cat. In addition, during one acute experiment, tests were also made using a commercially available impedance testing system (Custom Sound EP 2.0, Cochlear ltd, Sydney) and the results compared to faults identified by our system. Also, to ensure that faults could be identified by our system on a different array *in-vivo*, an experiment was performed with a pure platinum array implanted in the scala tympani of a cat and measurements were made with both our system and the commercial Custom Sound EP 2.0 system.

## 3. Results

### *3.1. RC circuit model-Testing and Validation*

The theoretical impedance values of the RC networks were compared to the experimentally obtained impedance values using the system (figure 4). The test pulse parameters used were 200 µA amplitude, 250 µs pulse width per phase with a 25 µs interphase gap. The optimal operating range of the system was found to be from 1 kΩ to 110 kΩ (using the test pulse parameters above) with an average percentage error of 3.24 % and a maximum percentage error of 10 % at 110 kΩ (figure 4). In order to measure impedances above 110 kΩ a test current of less than 200 µA was required to stay within stimulator compliance voltage.

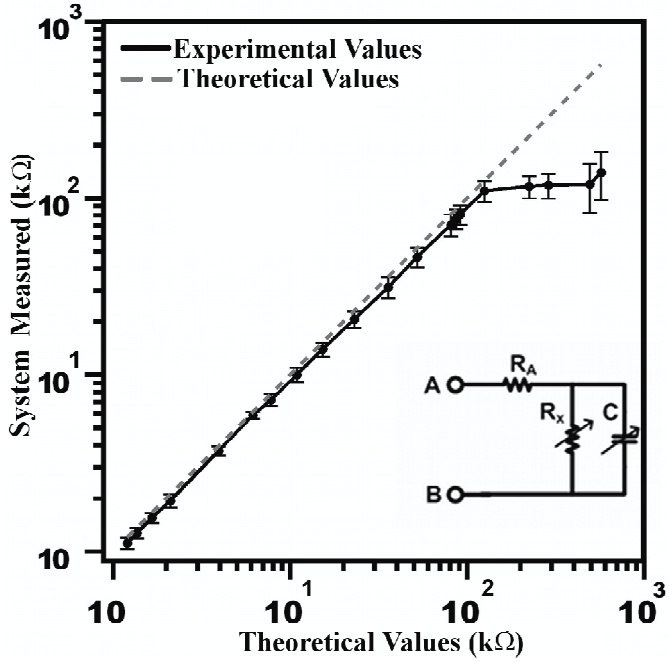


*Figure 4: A resistor-capacitor (RC) network was measured using system, and the values obtained were compared to the theoretical values of the RC combination at terminals 'A' and 'B' (inset).*

*Ten measurement trials were averaged for each RC combination. Error bars indicate standard error of the mean (SEM). Dashed line represents equal theoretical values and measured values by the system.*

The system performance at different currents (10-200μA) and pulse widths (50-1000μs) was evaluated with three RC combinations representing the lower (9.6 kΩ), middle (50 kΩ) and high (110 kΩ) range of the system (theoretical impedances were calculated using a 250 μs pulse). Figure 5A shows the plots of impedance normalized to the theoretical calculated value versus the current amplitude for each of the three impedance ranges. With all current amplitudes tested, impedance measurements were within 10% of the theoretical calculated values for all three impedance ranges. Figure 5B shows the impedance normalized to the theoretical calculated impedance versus the pulse width (50-1000 μs) for each of the three impedance ranges. Impedance values were found to be within 10% of the theoretical calculated values for all pulse widths with the middle impedance ranges, while for the low impedance range, only values measured using pulse widths > 100 μs, were within 10% of the theoretical calculated values. For the highest impedance range, although measurements were reasonably accurate within 10% error, only pulse widths less than 400 μs could be tested as the stimulator would reach compliance for longer pulse widths with the fixed current of 200 μA.

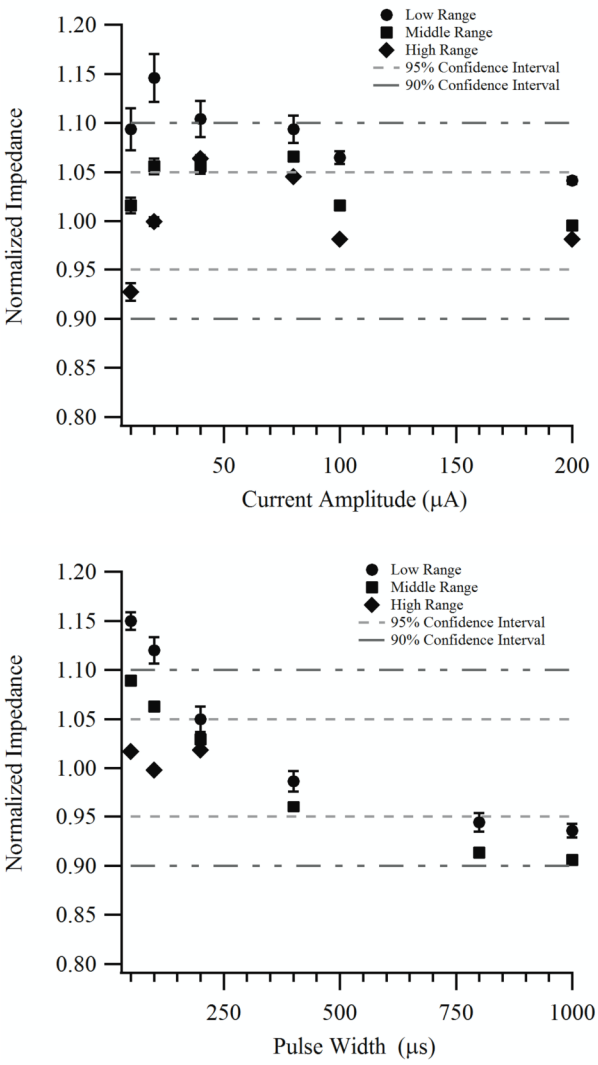


*Figure 5: System performance at different currents and pulse widths were evaluated with three RC combinations (Low-9.6 kΩ, Middle-50 kΩ, and High-110 kΩ) Theoretical impedance values were calculated using a 250 µs per phase pulse width. A) Normalized impedance versus current amplitude (10-200µA, pulse width was kept constant at 250µs). B) Normalized impedance versus pulse width (50-1000 µs, current was kept constant at 200 µA). For the highest impedance tested (110 kΩ) only values up to 200 µs are shown since the stimulator reached compliance for pulse widths greater than 400 µs. Error bars indicate the SEM.*

*3.2. In-vitro Analysis of Electrode Arrays*

Figure 6 shows the three electrode arrays used in this study (bottom panel) and the voltage waveforms (top panel) corresponding to each array. Table 2 shows the mean impedance of the three electrode arrays tested *in-vitro*. The test pulse parameters used were 200 µA amplitude, 250 µs pulse width per phase with a 25 µs interphase gap. As expected, measured impedances were found to correlate with electrode geometry (Electrodes with larger surface areas showed lower impedances; table 2).

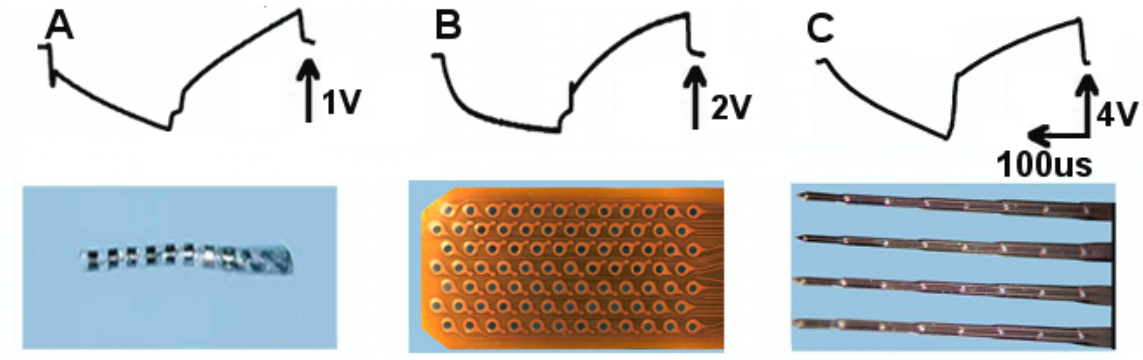


*Figure 6: Three types of multi-channel electrode arrays used for electrical stimulation applications in neural prostheses were tested in normal saline. The images show the array used and the corresponding voltage response waveforms across one of the electrodes on the array. A) Pure platinum array made up of 8 platinum rings on a silastic carrier. B) Platinum plated array made up of 84 electrodes arranged as a 7x12 array on a polyimide substrate and C) Iridium oxide array (NeuroNexus Technologies Inc.) made up of 32 electrodes arranged as a 4x8 array. A current pulse of 200 µA, 250 µs per phase with a 25 µs interphase gap was used to test each electrode array. Note: Different scales.*

**Table 2.** *In-vitro* analysis of electrode arrays using system.

| Electrode Name | Pure platinum array | Platinum plated array | Iridium oxide array |
|---|---|---|---|
| Designed | In-house | In-house | NeuroNexus Technologies Inc. |
| Manufactured | In-house (Shepherd et al., 1983) | Flexible Circuit Technologies (Plymouth, MN). plated in-house (Shivdasani et al., 2010) | NeuroNexus Technologies Inc. (Ann Arbour, MI). (Weiland and Anderson, 2000) |
| Number of sites | 8 | 84 | 32 |
| Geometric Surface Area | 430000 $\mu m^2$ | 123000 $\mu m^2$ | 413 $\mu m^2$ |
| Mean *in-vitro* Impedance | 3.3 kΩ | 11.6 kΩ | 80.80 kΩ |
| Standard Error of the Mean (SEM) | ±0.1 kΩ | ±1.3 kΩ | ±1.5 kΩ |
| Charge Transfer Mechanism | Pseudocapacitive | Pseudocapacitive | Reversible Faradiac |

The electrodes were found to exhibit different voltage waveform shapes. For example, the electrodes on the pure platinum array showed an initial step in voltage followed by a slower rise. In comparison, the electrodes of the platinum plated array did not show much of an initial step in voltage but showed a flatter second region than the other two arrays. The iridium oxide array had the largest peak voltage and showed a slow rising waveform with an almost constant slope.

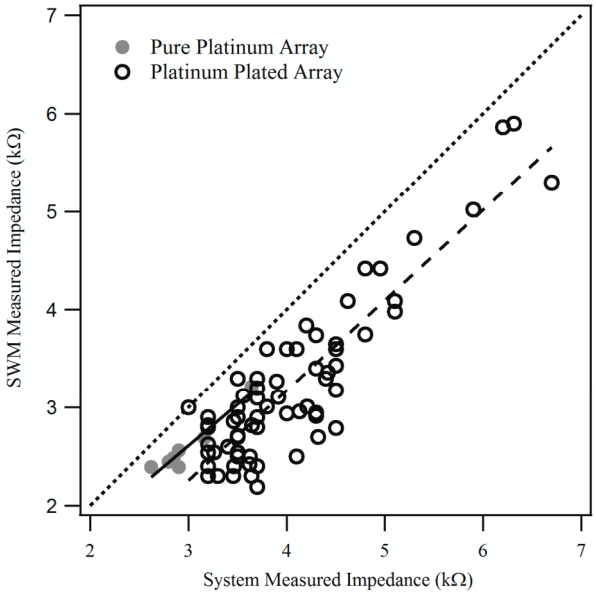


*Figure 7: Comparison of the impedance values obtained using the system described in the current work and the impedance values obtained using the SWM with a 4 kHz, 10 mV sine wave. The pure platinum array (8-electrodes, closed circles) and the platinum plated array (84-electrodes, open circles) were tested. A current pulse of 200 µA, 250 µs per phase with a 25 µs interphase gap was used to test each electrode array. Data points have been fitted using linear regression. Filled circles (solid line), $r^2$ = 0.9, slope = 0.84 and open circles (dashed line), $r^2$ = 0.78, slope = 0.92. Dotted line represents unity.*

Figure 7 shows a comparison of the impedances obtained from the pure platinum array and the platinum plated array using the system described here and those obtained using the SWM. The impedances obtained from the two methods were comparable in value with our system generally tending to measure slightly higher impedance values than those obtained using the SWM (figure 7).

*3.3 In-vivo Analyses.*

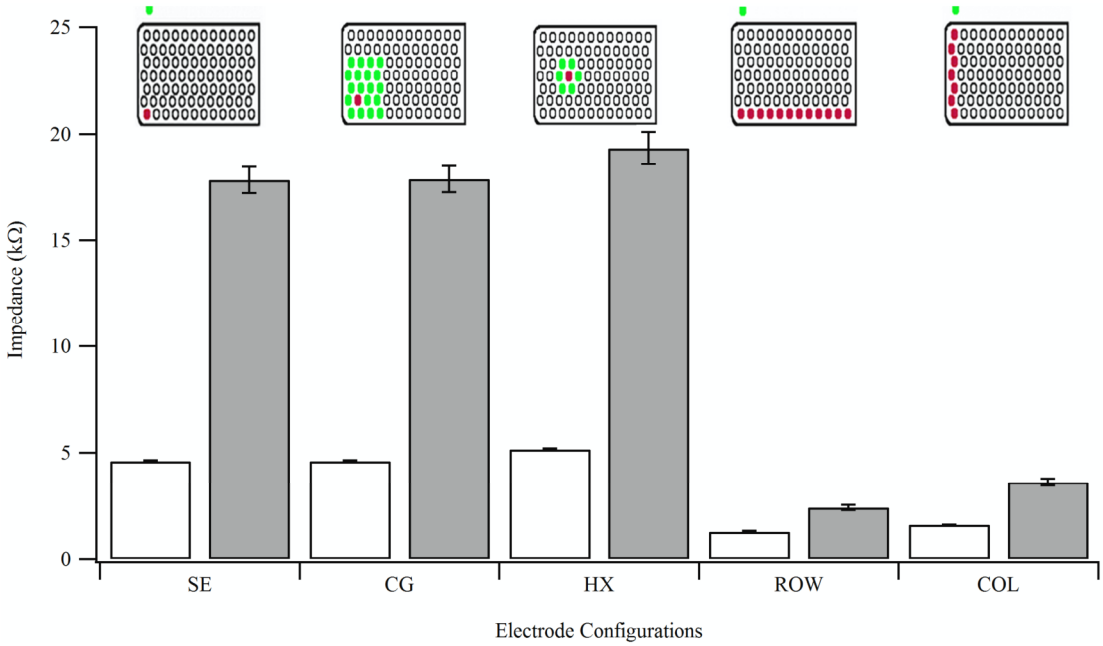


*Figure 8: The in-vitro (open bars) and in-vivo (filled bars) impedances of the platinum plated array was analysed for specific stimulation configurations (see figure 2). The in-vivo values show an increase in impedance from the in-vitro values for all stimulation configurations. A 200µA (250µs per phase and 25µs interphase gap) stimulation current pulse used for impedance analysis (see figure 3A).*

Figure 8 shows the mean *in-vitro* and *in-vivo* impedances of the platinum plated array (bars) in each stimulation configuration (top). The *in-vivo* impedance measured immediately after implantation was found to increase by a factor of 1.5-2.5 times the *in-vitro* impedance measured in normal saline prior to implantation. The system measured the impedances of all the electrodes on each array in less than 10 seconds in the monopolar configuration while speeds using other configurations varied (table 3). The configuration was also found to affect the impedance values measured. Impedances measured using the SE and CG configurations were similar however they

were lower than those measured using the HX configuration. The ROW and COL configurations showed the lowest measured impedances.

**Table 3.** System temporal performance in scanning the 7 x 12 platinum plated array.

| *Electrode Configuration on the Platinum plated array* | *Number of electrodes connected as Active for each measurement* | *Number of electrodes connected as Return for each measurement* | *Number of electrodes tested* | *Time taken to scan the whole array* |
|---|---|---|---|---|
| *SE* | *1* | *1* | *84* | *<10 s* |
| *CG* | *1* | *19* | *84* | *<20 s* |
| *HX* | *1* | *6* | *67* | *<15 s* |
| *ROW* | *12* | *1* | *12* | *<5 s* |
| *COL* | *7* | *1* | *7* | *<5 s* |

### *3.4. Fault detection*

The system reliably detected all the fabricated faults on the platinum plated array in less than 20 seconds *in-vitro*. Short circuited electrodes showed very low impedances with no voltage response waveform as shown in figure 3C. Open circuited electrodes showed very high impedances and a characteristic waveform as shown in figure 3D. Normal working electrodes with no faults showed a characteristic waveform as shown in figure 3B. In 20 *in-vivo* experiments performed with the platinum plated array, several open circuits and 3 short circuits were detected - these were later confirmed to be caused by wiring errors or trauma to the array during implantation. In the scala tympani experiment, only one open circuit was detected – this was determined to be caused by a lead-wire breakage. When tested *in-vivo*, identical faults were detected with both our system and the Custom Sound EP 2.0 system. The platinum plated array had one open circuit and one short

circuit and the pure platinum array had one open circuit. In all the tests conducted, there were no false positives in the results and the existence of faults did not change the scanning speeds (table 3).

## 4. Discussion

The present study describes a system and method for rapid evaluation of high density electrode arrays including effective mapping of stimuli to multiple electrodes on the array, estimation of the instantaneous impedance of the electrode-tissue interface and quick and reliable electrode fault detection. The system reliably performed fast *in-vitro* and *in-vivo* measurements over a wide range of impedances and with a range of electrode arrays. In addition, the system accurately identified all open and short circuit faults when tested.

### *4.1 System Performance*

Using different RC network circuits which model the electrode-tissue interface, we were able to determine a working impedance range for the system. Using a 200 µA, 250 µs per phase current pulse, a maximum impedance of 110 kΩ could be measured within 10% error. In addition, the system made accurate impedance measurements within 10% error at all current levels between 50-200 µA and at pulse widths greater than 200 µs for a wide range of impedances. The upper limits were primarily due to the compliance voltage of the stimulator (24V). A higher compliance voltage may improve the measurement ranges and accuracy even further (see section below on Alternative Design).

Our system was effective in measuring impedances of several types of arrays with electrodes of different sizes and materials using the SWT. The results obtained were comparable to those measured using the SWM with a commercially available testing system. However, our system made use of a simple two-electrode set up for impedance measurements while the SWM required an additional reference electrode for measurements. In addition, the constant current stimulator used in our system eliminated the need for voltage protection circuitry, which is often required when using the SWM (Gunalan et al., 2009). These attributes give our system the advantage of

being readily used in a clinical setting where a standard reference electrode is not available.

Of the three arrays that were tested *in-vitro*, the pure platinum array had the lowest impedance and the iridium oxide array had the highest impedance. The difference in impedance was mainly attributed to the difference in the GSA of the electrodes. It must be noted that the area considered here was only the GSA, however the electrochemical surface area also plays a role in the impedance of porous electrodes such as those on the platinum plated array and the iridium oxide array. Generally however, the electrochemical surface area is difficult to determine and not often reported (Cogan, 2008). There were also significant differences in the characteristic voltage waveforms for each array, these could be attributed to several reasons including the electrode area (both the GSA and the electrochemical surface area), the interface (normal saline/tissue), the charge transfer mechanism (Table 3) and the resultant electrochemical reactions involved during stimulation (Tykocinski et al., 2005, Weinman and Mahler, 1964, Cogan, 2008). The exact cause of the changes in voltage waveforms across electrode arrays could not be determined by the experiments performed in this study.

Impedances were obtained using the platinum plated array in several electrode configurations including monopolar, common ground and hexagonal returns *in-vitro* and *in-vivo*. The impedances of the electrodes were found to be affected by the number of active electrodes and the number of electrodes comprising the return electrode in each configuration. In the SWT the voltage is measured using a two-electrode setup, therefore the measured impedance is the result of the combined impedance of the active and return electrodes. In the monopolar configurations (SE, ROW and COL) the return electrode was a platinum ball electrode with very low impedance (350 Ω); hence the impedance of the return electrode had very little effect on the measured impedance. The HX and CG configurations were made of a return electrode comprising of 6 and 19 electrodes

shorted together respectively. . Hence with the HX and CG configurations, impedances measured were slightly higher than those measured with the SE configuration. Furthermore, the ROW and COL configurations had much lower impedances than the other configurations measured because the active electrode comprised of 12 and 7 electrodes shorted together respectively, thereby increasing the GSA of the active electrode. Finally, the system was able to detect common faults such as open and short circuits, both replicated in the laboratory and in real world applications at a similar performance level to the Custom Sound EP 2.0 commercial system.

The system provided fast scanning of electrodes on high density electrode arrays in all configurations. The speed of scanning depended on the NI-2532 relay operating time (0.25 ms); DMM initialisation time (4 ms); number of simultaneous switch connections for different electrode configurations; and the pulse width of the constant current pulse. For example in the monopolar SE configuration, 4 simultaneous switch connections were required (two for the stimulator and two for the DMM to record the voltage waveform), while in the CG configuration, 40 simultaneous switch connections were required to connect 20 electrodes (1 active and 19 return) and record from them. The system was able to scan up to 84 electrodes in the monopolar SE configuration in less than 10 seconds and in the CG configuration in less than 20 seconds; using the standard test pulse parameters of 200 μA, 250 μs per phase, 25 μs inter phase gap. Furthermore, the identification of electrode faults did not change scanning speeds.

*4.2 System Applications*

The method and system described in the current work could be applied to both stimulating and recording electrodes in both a clinical and experimental setting. Chronic recording electrodes such as the ones used in neural interfaces (eg. Brain machine interfaces-BMIs) can be potentially tested

using such a system to characterize tissue reactions and perform *in-vivo* calibration. This system can be used with EEG based BMI's that employ electrodes with impedances in the 1-110 kΩ range. Currently available BMI's use up to 100 electrodes on an array and higher density arrays could be employed in the future. Routine evaluation of such arrays *in-vivo* will thus become important to ensure the effectiveness of chronic BMI's. Chronic stimulating electrodes such as the ones used in auditory, visual, motor and other neural prostheses can also use this method for evaluating electrode performance; detecting tissue and electrode damage; measurement of impedances and detection of faults. Furthermore, this method can also obtain a better understanding of the charge transfer mechanism involved during chronic stimulation (Brummer et al., 1983, Rose and Robblee, 1990, Shepherd et al., 1990, Newbold et al., 2004). Particularly where the high density electrode arrays are concerned, this method enables a quick and safe evaluation of the array both *in-vitro* and *in-vivo*.

### *4.3 Errors and Limitations*

The system was limited by the consecutive switching capability of the switch matrix and an impedance measurement range of less than 110 kΩ. Further, the use of very low currents and very long pulse widths affected the system performance in impedance measurements. The NI-4532 switch matrix can only connect 40 switches simultaneously, which effectively reduced the number of electrodes that could be connected simultaneously, especially in the CG configuration. The current waveform measurements were limited by the DMM's accuracy in measuring currents less than 200 µA, while the stimulator compliance voltage was a limiting factor for measurements using longer pulse widths and large current amplitudes, particularly with the high impedance range. Furthermore, parasitic capacitances and resistances from the DMM, switch and cables affected

measurements at high impedances (greater than 110 kΩ) and at very low currents. Noise induced errors also contributed to measurement errors at low currents and with high impedance electrodes.

*4.4 Alternative design*

Despite some shortcomings, the SWT-based system described in this study is versatile and can accommodate various types of electrode arrays with little or no modifications required to the hardware. The switches can also be easily expanded to address arrays with greater numbers of electrodes than those described in this study. The accuracy and range of the system can be further improved by applying adequate compensation for the parasitic capacitances and resistances as well as by using a constant current stimulator with a larger voltage compliance, or by using current levels <200 μA. For example a constant current stimulator with a voltage compliance of 100V can measure impedances up to 1 MΩ using a 200 μA current pulse and using a 10 μA current pulse this range can be increased up to 2.4 MΩ. If desired, this system can be easily adapted for use with the SWM by replacing the constant current stimulator with a sine wave generator. The effects of capacitive coupling in the cables and noise at low currents can be reduced by using shielded cables and by replacing the DMM used to measure current with one which is more sensitive.

## 5. Conclusions

The system and method described measured the impedance of several electrode arrays reliably, both *in-vitro* and *in-vivo* in the 1 kΩ to100 kΩ range in several electrode configurations, with fast scanning speeds, reasonable accuracy and correct identification of faults. Together the results indicate that this approach is capable of rapid evaluation of a range of high density electrode arrays both *in-vitro* and *in-vivo* and can be very beneficial in a clinical environment.

**Acknowledgements**

The authors wish to thank Penny Allen for assistance with surgeries, Mark Harrison and David Ng for designing the flexible electrode arrays. This work was performed at the Bionic Ear Institute at St Vincent’s hospital. Funding was provided by the Ian Potter Foundation, John T Reid Charitable Trusts and Bionic Vision Australia’s Special Research Initiative "Research in Bionic Vision Science and Technology" from the Australian Research Council. The Bionic Ear Institute wishes to acknowledge the supported of the Victorian Government through its Operational Infrastructure Support Program.

**References**

Brindley G S and Lewin W S (1968) The sensations produced by electrical stimulation of the visual cortex. *J Physiol* **196**:479-93

Brummer S B, Robblee L S and Hambrecht F T (1983) Criteria for selecting electrodes for electrical stimulation: theoretical and practical considerations. *Ann N Y Acad Sci* **405**:159-71

Brummer S B and Turner M J (1977) Electrochemical considerations for safe electrical stimulation of the nervous system with platinum electrodes. *IEEE Trans Biomed Eng* **24**:59-63

Clark G M (2003) *Cochlear implants : fundamentals and applications / Graeme Clark* Editor Place New York : Springer

Cogan S F (2006) In vivo and in vitro differences in the charge-injection and electrochemical properties of iridium oxide electrodes *Journal* **1** 882-5

Cogan S F (2008) Neural Stimulation and Recording Electrodes. *Annual Review of Biomedical Engineering* **10**:275-309

Cogan S F (2008) Neural stimulation and recording electrodes. *Annu Rev Biomed Eng* **10**:275-309

Donoghue J P (2008) Bridging the brain to the world: a perspective on neural interface systems. *Neuron* **60**:511-21

Dymond A M (1976) Characteristics of the metal-tissue interface of stimulation electrodes. *IEEE Trans Biomed Eng* **23**:274-80

Gunalan K, Warren D J, Perry J D, Normann R A and Clark G A (2009) An automated system for measuring tip impedance and among-electrode shunting in high-electrode count microelectrode arrays. *J Neurosci Methods* **178**:263-9

Hornig R, Laube T, Walter P, Velikay-Parel M, Bornfeld N, Feucht M, Akguel H, Rossler G, Alteheld N, Lutke Notarp D, Wyatt J and Richard G (2005) A method and technical equipment for an acute human trial to evaluate retinal implant technology. *J Neural Eng* **2**:S129-34

Humayun M S, De Juan E, Jr., Weiland J D, Dagnelie G, Katona S, Greenberg R and Suzuki S (1999) Pattern electrical stimulation of the human retina. *Vision Res* **39**:2569-76

Mccreery D, Lossinsky A, Pikov V and Liu X (2006) Microelectrode array for chronic deep-brain microstimulation and recording. *IEEE Trans Biomed Eng* **53**:726-37

Mercanzini A, Colin P, Bensadoun J C, Bertsch A and Renaud P (2009) In vivo electrical impedance spectroscopy of tissue reaction to microelectrode arrays. *IEEE Trans Biomed Eng* **56**:1909-18

Middlebrooks J C and Snyder R L (2008) Intraneural stimulation for auditory prosthesis: modiolar trunk and intracranial stimulation sites. *Hear Res* **242**:52-63

Mushahwar V K, Collins D F and Prochazka A (2000) Spinal cord microstimulation generates functional limb movements in chronically implanted cats. *Exp Neurol* **163**:422-9

Newbold C, Richardson R, Huang C Q, Milojevic D, Cowan R and Shepherd R (2004) An in vitro model for investigating impedance changes with cell growth and electrical stimulation: implications for cochlear implants. *Journal of Neural Engineering* **1**:218-27

Newbold C, Richardson R, Huang C Q, Milojevic D, Cowan R and Shepherd R (2004) An in vitro model for investigating impedance changes with cell growth and electrical stimulation: implications for cochlear implants. *J Neural Eng* **1**:218-27

Parker J R, Duan Y Y, Patrick J, Harrison H B, Reinhold O and Clark G M (1999) *Testing of thin-film electrode arrays for cochlear implants of the future* Editor Place

Prochazka A and Mushahwar V K (2004) *Spinal Cord and Rootlets* In: *Neuroprosthetics Theory and Practice* Horch, K W and Dhillon, G S Place Singapore World Scientific 786-806

Rizzo J F, 3rd, Wyatt J, Loewenstein J, Kelly S and Shire D (2003) Perceptual efficacy of electrical stimulation of human retina with a microelectrode array during short-term surgical trials. *Invest Ophthalmol Vis Sci* **44**:5362-9

Rose T L and Robblee L S (1990) Electrical stimulation with Pt electrodes. VIII. Electrochemically safe charge injection limits with 0.2 ms pulses. *IEEE Trans Biomed Eng* **37**:1118-20

Schwartz A B (2004) Cortical neural prosthetics. *Annu Rev Neurosci* **27**:487-507

Seligman P M and Shepherd R K (2004) *Cochlear Implants* In: *Neuroprosthetics: Theory and Practise* Hoch, K and Dhillon, G Place Singapore World Scientific 878-904

Shah S, Hines A, Zhou D, Greenberg R J, Humayun M S and Weiland J D (2007) Electrical properties of retinal-electrode interface. *J Neural Eng* **4**:S24-9

Shepherd R K, Clark G M and Black R C (1983) Chronic electrical stimulation of the auditory nerve in cats. Physiological and histopathological results. *Acta Otolaryngol Suppl* **399**:19-31

Shepherd R K, Franz B K-H and Clark G M (1990) *The biocompatibility and safety of cochlear prostheses* In: *Cochlear Prostheses* Clark, G M, Tong, Y C and Patrick, J F Place Melbourne Churchill Livingstone 69-98

Shivdasani M N, Luu C D, Cicione R, Fallon J B, Allen P J, Leuenberger J, Suaning G J, Lovell N H, Shepherd R K and Williams C E (2010) Evaluation of stimulus parameters and electrode geometry for an effective suprachoroidal retinal prosthesis. *J Neural Eng* **7**:036008

Suaning G J, Hallum L E, Preston P J and Lovell N H (2004) An efficient multiplexing method for addressing large numbers of electrodes in a visual neuroprosthesis. *Conf Proc IEEE Eng Med Biol Soc* **6**:4174-7

Suaning G J, Hallum L E, Preston P J and Lovell N H (2004) An efficient multiplexing method for addressing large numbers of electrodes in a visual neuroprosthesis *Journal* **6** 4174-7

Suner S, Fellows M R, Vargas-Irwin C, Nakata G K and Donoghue J P (2005) Reliability of signals from a chronically implanted, silicon-based electrode array in non-human primate primary motor cortex. *IEEE Trans Neural Syst Rehabil Eng* **13**:524-41

Teorell T (1946) Application of "Square Wave Analysis" to Bioelectric Studies. *Acta Physiologica Scandinavica* **12**:235-54

Tykocinski M, Cohen L T and Cowan R S (2005) Measurement and analysis of access resistance and polarization impedance in cochlear implant recipients. *Otol Neurotol* **26**:948-56

Weiland J D and Anderson D J (2000) Chronic neural stimulation with thin-film, iridium oxide electrodes. *IEEE Trans Biomed Eng* **47**:911-8

Weinman J and Mahler J (1964) An Analysis of Electrical Properties of Metal Electrodes. *Med Electron Biol Eng* **2**:299-310

Xinyu C, Liming L, Kaijie W, Chuanqing Z, Pengjia C and Qiushi R (2008) C-Sight Visual Prostheses for the Blind. *IEEE Engineering in Medicine and Biology Magazine* **27**:20-8

Xu J, Shepherd R, Millard R and Clark G (1997) Chronic electrical stimulation of the auditory nerve at high stimulus rates: a physiological and histopathological study. *Hearing research* **105**:1-29

Xu J, Shepherd R K, Millard R E and Clark G M (1997) Chronic electrical stimulation of the auditory nerve at high stimulus rates: a physiological and histopathological study. *Hear Res* **105**:1-29

Zrenner E, Bartz-Schmidt K U, Benav H, Besch D, Bruckmann A, Gabel V P, Gekeler F, Greppmaier U, Harscher A, Kibbel S, Koch J, Kusnyerik A, Peters T, Stingl K, Sachs H, Stett A, Szurman P, Wilhelm B and Wilke R (2010) Subretinal electronic chips allow blind patients to read letters and combine them to words. *Proceedings of the Royal Society B: Biological Sciences*

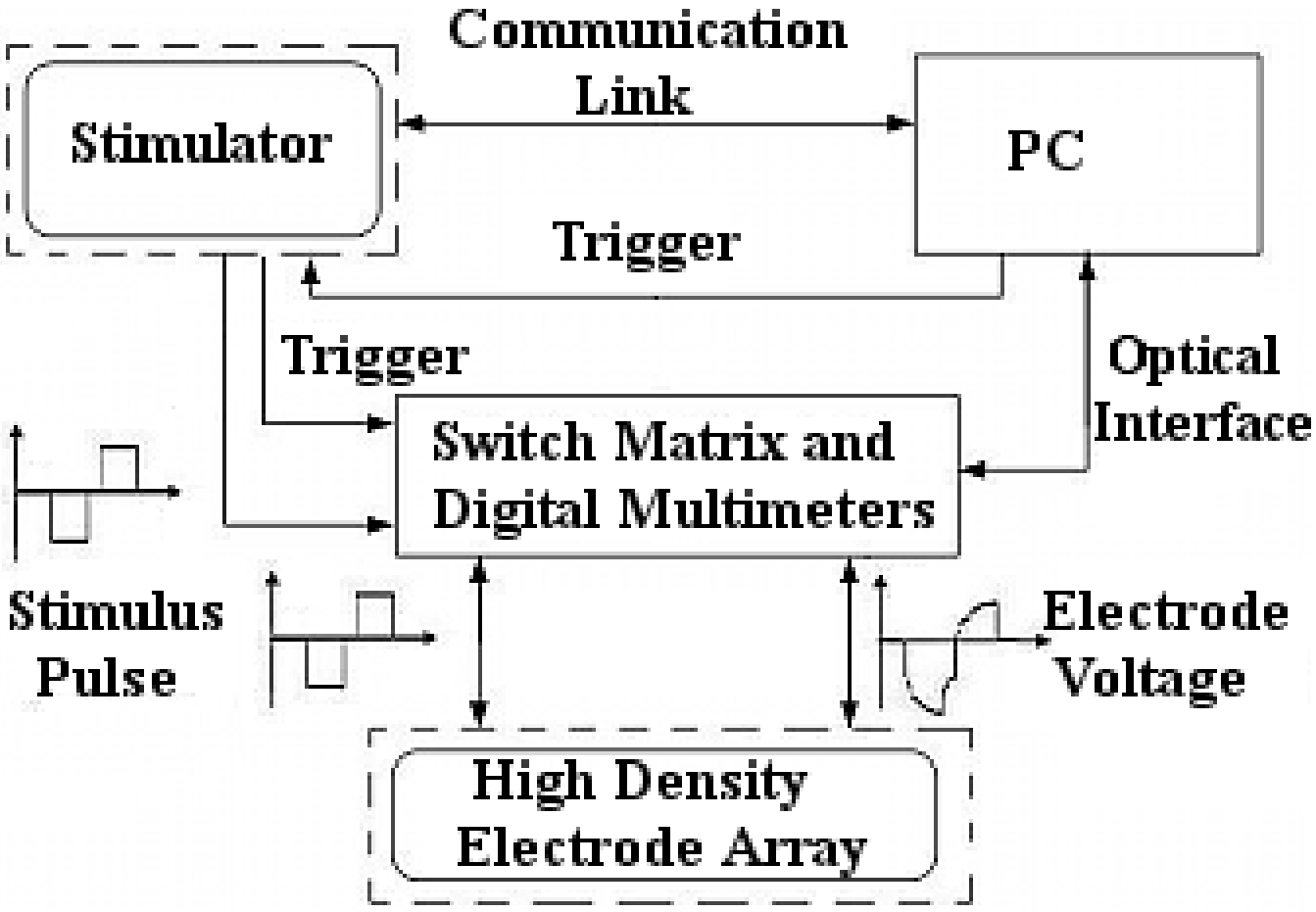


**Figure 1 (Figure1.tiff)**

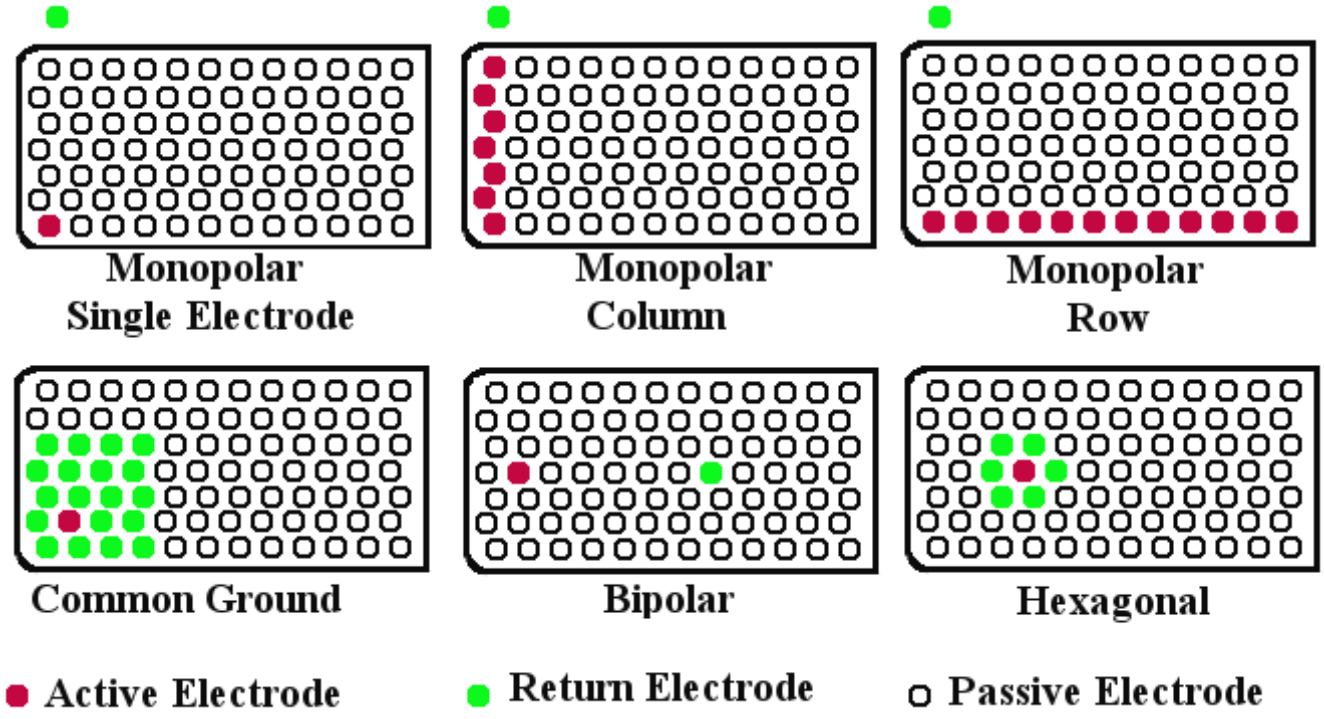


**Figure 2 (Figure2.tif)**

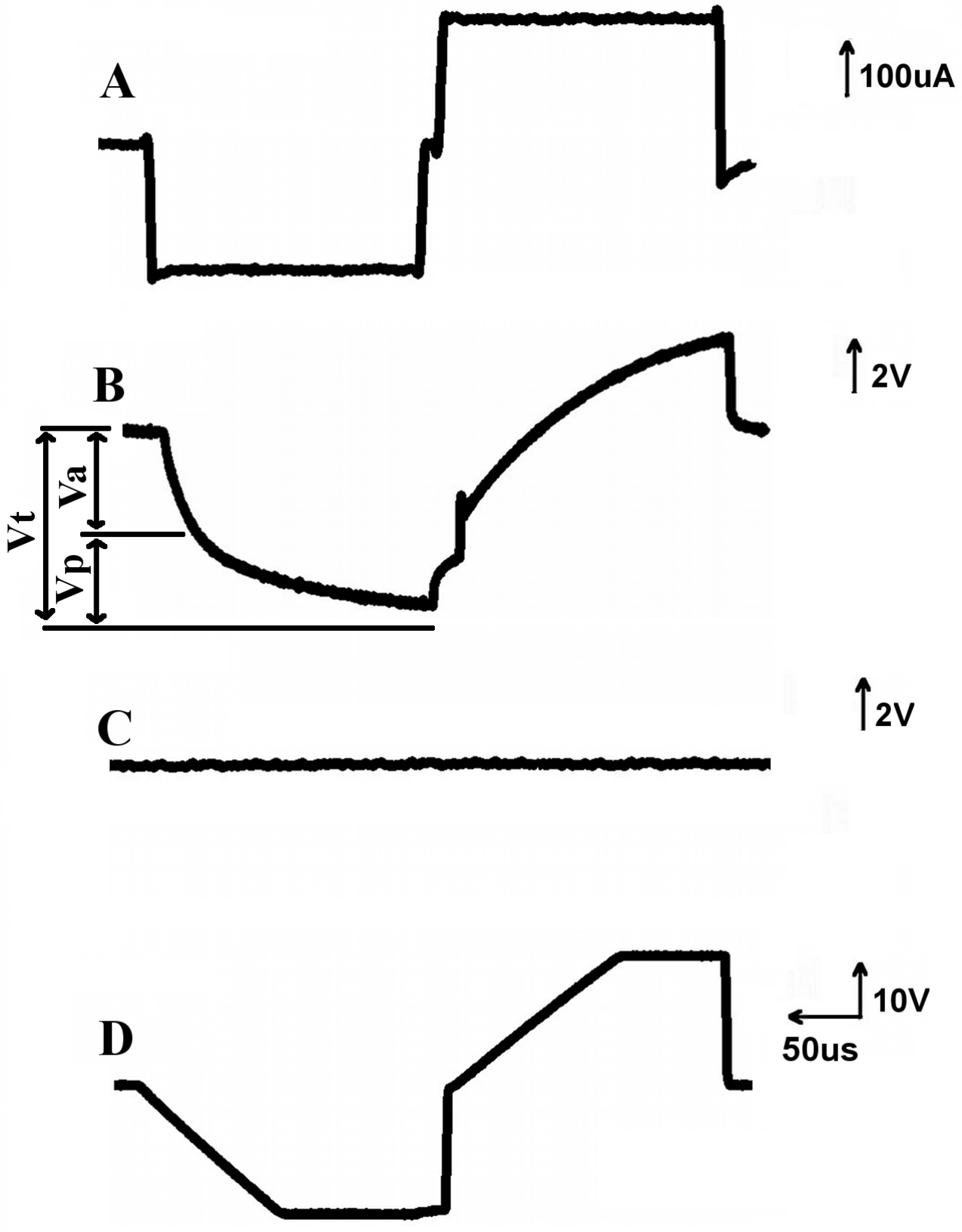


**Figure 3 (Figure3.tiff)**

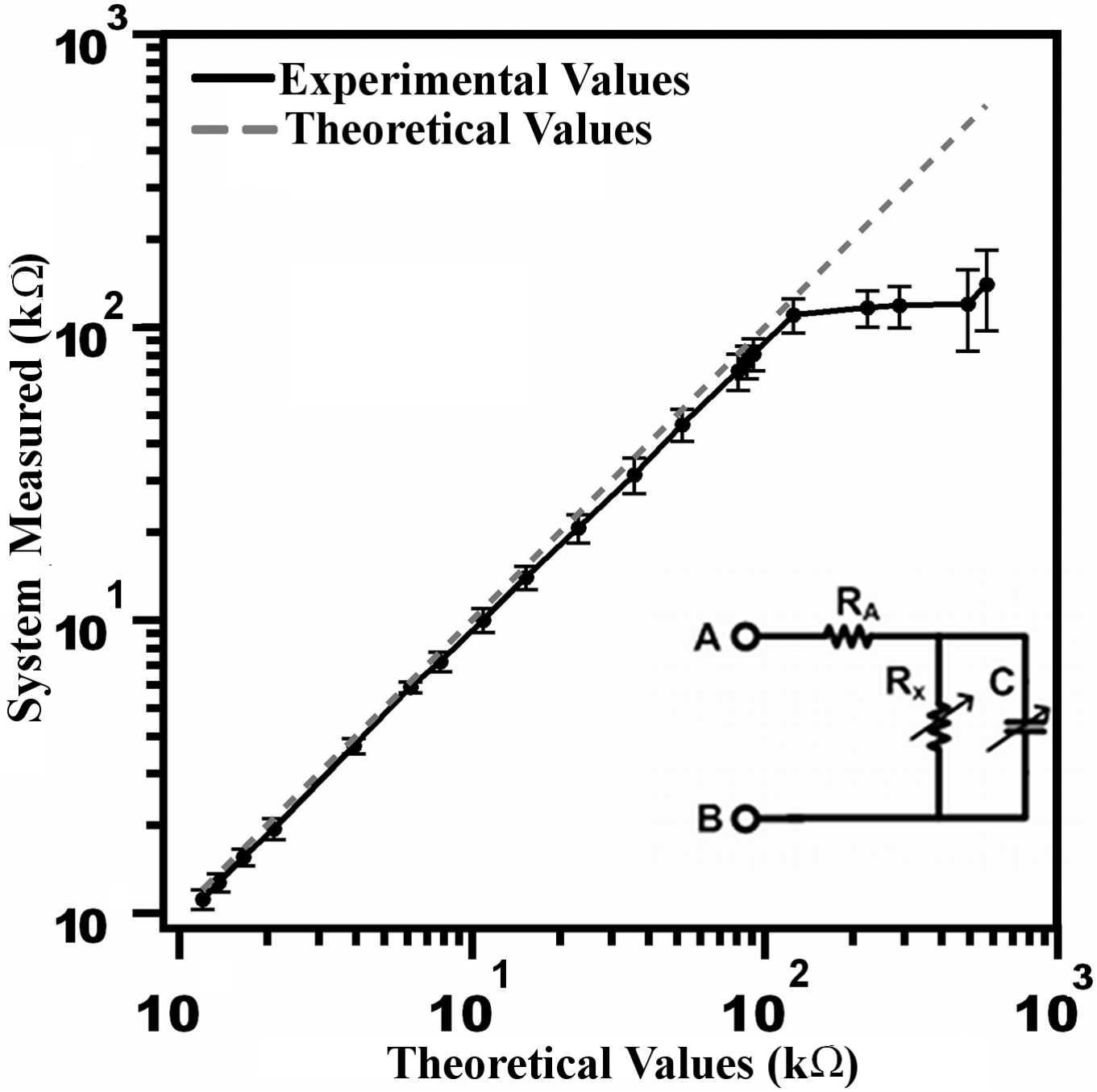


**Figure 4 (Figure4.tiff)**

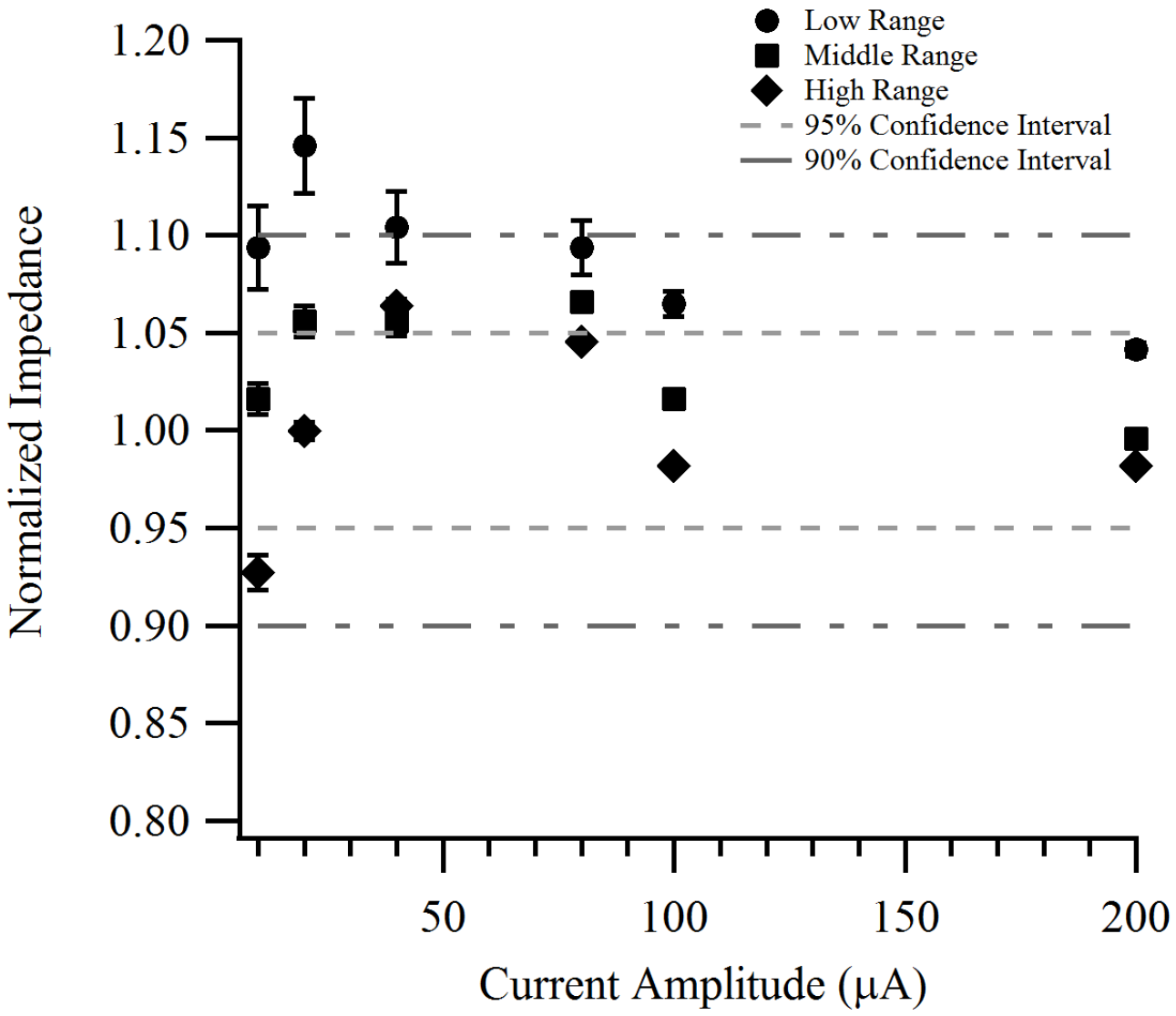


**Figure 5a (Figure5a.tif)**

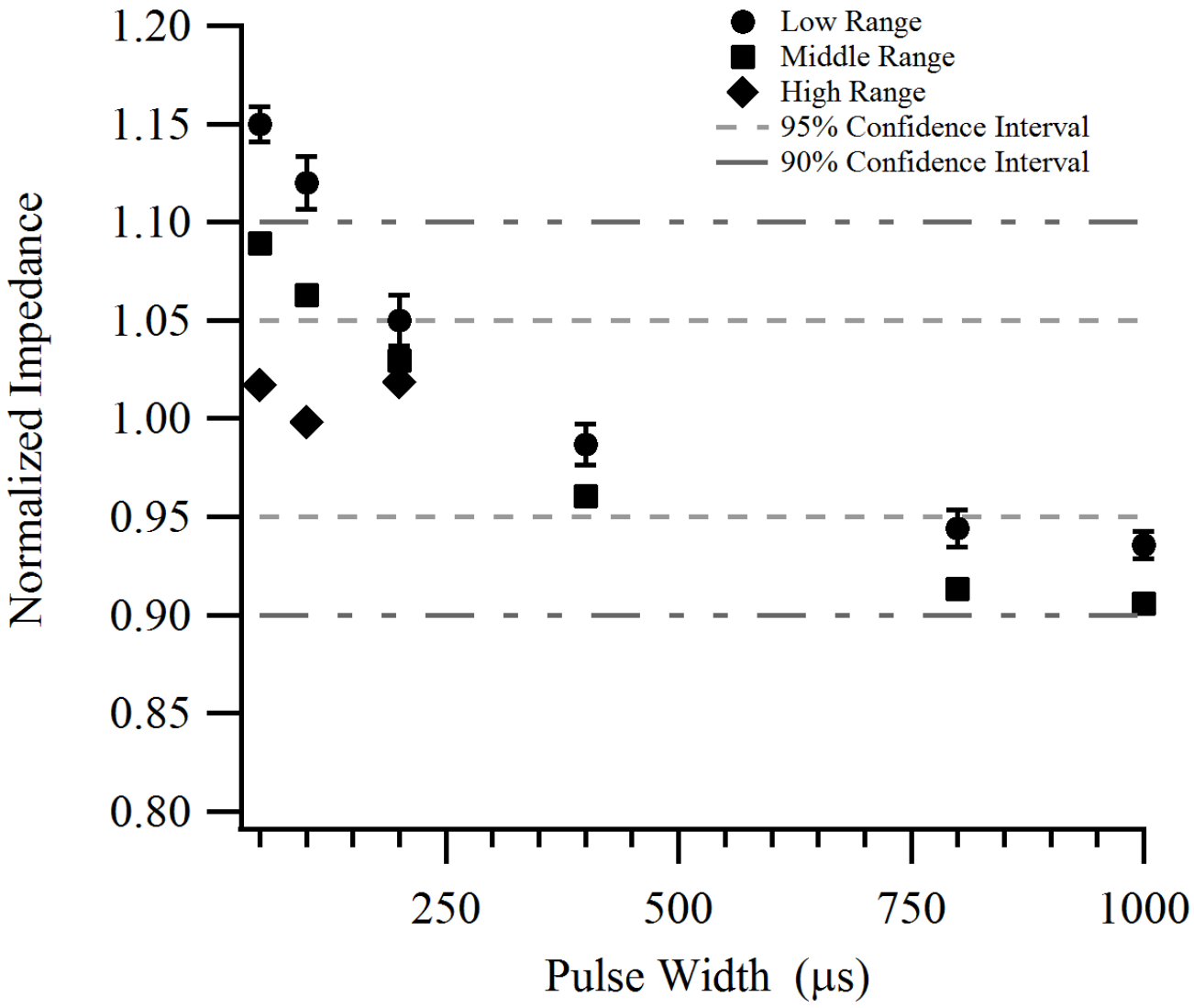


**Figure 5b (Figure5b.tif)**

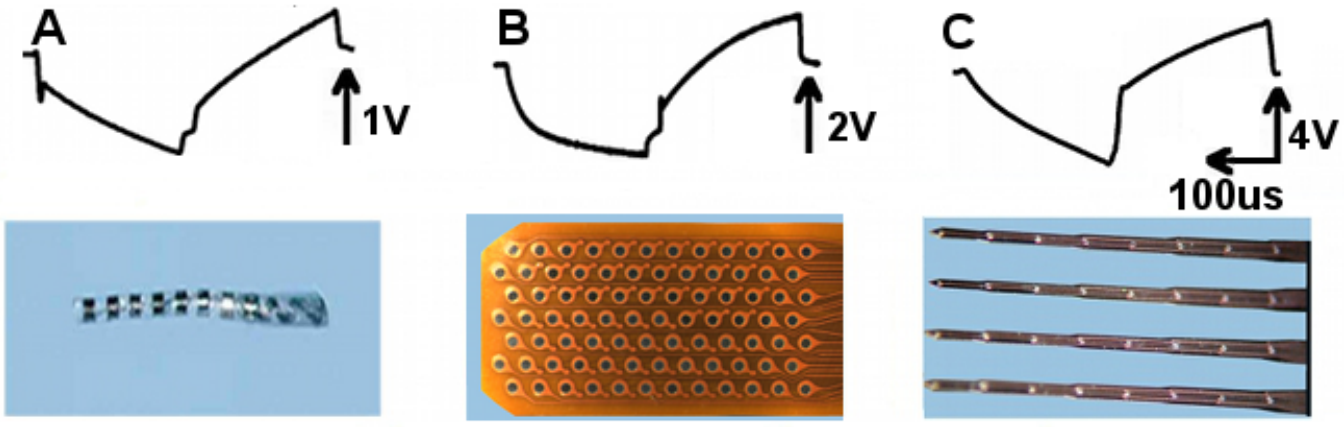


**Figure 6 (Figure6.tiff)**

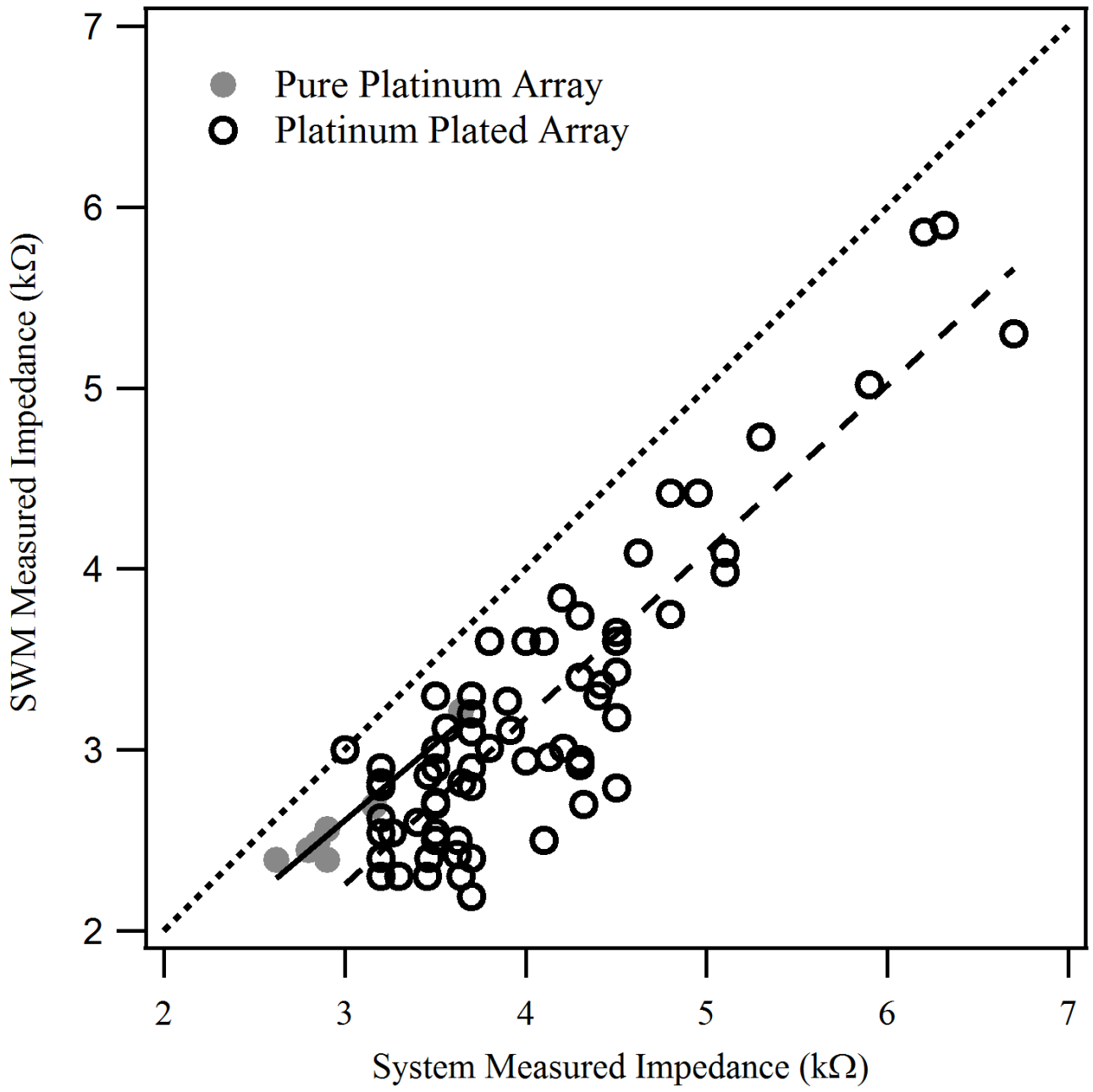


**Figure 7 (Figure7.tif)**

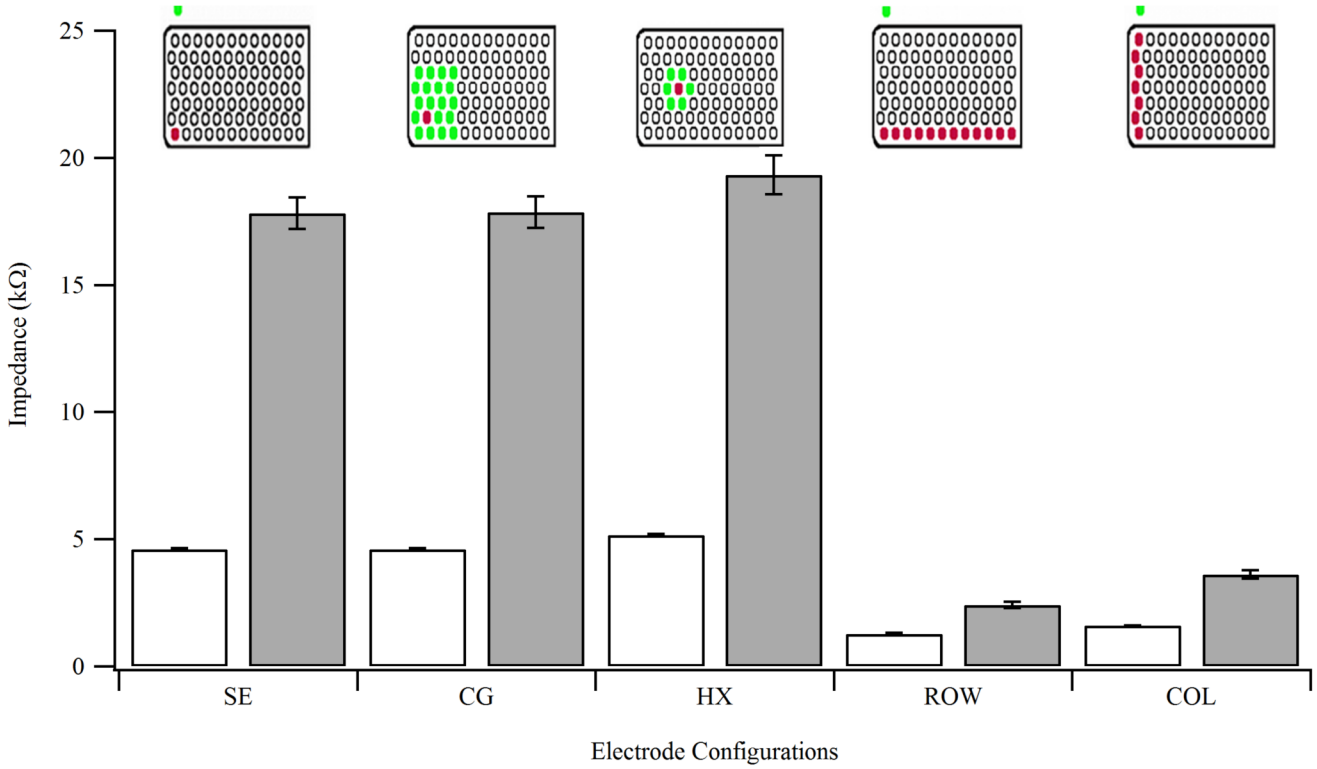


**Figure 8 (Figure8.tif)**